JOURNAL OF MATERIALS SCIENCE: MATERIALS IN MEDICINE **14** (2003) 605–610

Amorphous alloys resistant to corrosion in artificial saliva solution

A. KWOKAL, M. METIKOŠ-HUKOVIĆ*
Department of Electrochemistry, Faculty of Chemical Engineering and Technology, University of Zagreb, P.O. Box 177, 10 000 Zagreb, Croatia
E-mail: mmetik@marie.fkit.hr

N. RADIĆ
Institute Ruđer Bošković, 10 000 Zagreb, Croatia

R. POLJAK-GUBERINA, A. ČATOVIĆ
School of Dental Medicine, University of Zagreb, 10 000 Zagreb, Croatia

The tailoring of new corrosion-resistant alloys with specific properties has recently been performed mostly by the sputter deposition technique. The aim of this work was to investigate corrosion resistance of aluminum–tungsten (Al–W) amorphous alloys in artificial saliva solution, pH = 5.5, based on the electrochemical methods of cyclic voltammetry and linear polarization. Thin alloy films were prepared on a sapphire substrate by magnetron codeposition. Completely amorphous films were obtained in the $Al_{80}W_{20}$–$Al_{67}W_{33}$ composition range. Amorphous Al–W alloys exhibit very high corrosion resistance due to their homogeneous single-phase nature. The passive films spontaneously formed at their surface are uniform with characteristics of an insulator film and prevent corrosion progression in the bulk in a very demanding oral environment. The mechanism of increasing resistivity of Al–W alloys to pitting corrosion and generalized corrosion has been discussed in the view of increasing tungsten content in the alloy. Considering these exceptional corrosion properties and microhardness which falls in the range 7.5 ± 1.6 Pa, Al–W alloys represent promising materials for dental applications.

1. Introduction

A wide range of various alloys is used in dental prosthetics. In choosing the metal materials for mouth prosthetics, special attention must be paid to their corrosion resistance – the main condition governing biocompatibility of materials in the biological surroundings of the mouth. Economical reasons are the causes of expanding use of alloys in everyday applications. The resistance of these alloys to corrosion is often insufficient, which negatively influences the durability of the prosthetic device inside the mouth, and the condition of the mouth linings. *In vitro* investigations have shown that each alloy immersed in saliva releases metal ions, generating a protective biofilm at the alloy | saliva boundary, which protects the alloy from further dissolution (corrosion) [1]. Increasing the concentration of proteins and glycoproteins in the saliva increases the rate of generation of the protective biofilm and decreases the corrosion activity of the metal inside the mouth [2, 3]. The most common is the sulfide biofilm, which forms as a consequence of metal sulfide generation by the reaction of the alloy and sulfur from the consumed food and drinks [4]. *In vivo* investigations gave different results. Due to constant circulation of the saliva, the protective biofilm gets degraded and dissolution of the metal is continual. Mastication helps the degradation process of the biofilm. Lian and Melitis [5] have shown that dental works exposed to friction forces during mastication corrode much faster in comparison to those not exposed to friction. This is why the biofilm does not satisfactorily protect the metal from further corrosion, rather, it only slows down its corrosion activity.

This paper investigates the corrosion properties of amorphous Al–W coatings for dental applications, deposited on a ceramic substrate in artificial saliva, pH = 5.5. ''Metallic glasses'', ''glassy metals'', and ''amorphous metals'' are synonyms used for amorphous alloys [6, 7]. The term ''metal'' assumes conductivity similar to that observed in solid or liquid metals, while ''glass'' refers to the amorphous metal obtained by sudden cooling of the melt. Of all the chemical properties, significant attention has been paid to corrosion resistance, as well as oxidation and catalytic properties of the amorphous alloys [8]. Due to their composition and amorphous structure, metallic glasses exhibit very high corrosion resistance, most of the time

---

*Author to whom all correspondence should be addressed.

0957–4530

greater than that exhibited by crystalline alloys of the same composition [9, 10].

Electrochemical theory describes metal corrosion as a combination of the anodic metal dissolution reaction where metal ions are the products, and the cathodic reduction reaction, such as oxygen ionization and discharge of hydrogen ions [11]. In order to understand the corrosion properties of amorphous alloys, it is important to be familiar with the electrochemical theory of passivation of metals and alloys. Although electrochemical passivation is a general phenomenon which may be observed on all metals, the majority of investigations related to the passivity of biocompatible alloys-implants in simulated physiological solutions deals with titanium and its alloys [12–17], CoCrMo [18–20] and stainless steel [21, 22]. The passivation of metals and alloys is described as a change in the kinetics of the electrode reaction (dissolution) due to adsorption of oxygen species and formation of a new oxide phase (hydroxide) whose thickness ranges from one monolayer to several nanometers [23, 24]. Nonstoichiometric oxide films form on the surface of valve metals including Al and W (in addition to Ta, Ti, V, Zr and others), which are characterized by the tendency to self-passivate in contact with the oxygen from air or water. In contrast to the stoichiometric oxide, which may be represented by the general formula $\mathrm{MO}_{n/2}$, the nonstoichiometric oxide has a general formula $\mathrm{MO}_{n/2\pm x}$, where n is the charge on the metal, and x depends on the contribution of anionic $(-x)$ and cationic $(+x)$ vacancies. According to the point defect model (PDM), the growth of a passive oxide film takes place via movement (migration or diffusion) of anion vacancies, [24], which are positively charged and/or cation vacancies, $V_{\mathrm{M}}^{\chi'}$, which are negatively charged, through the oxide film.

Thin films of amorphous aluminum and tungsten alloys represent new perspective materials which exhibit exceptional chemical and physical properties; stability in chemically aggressive surroundings and at elevated temperatures [25–27], adhesion to the substrate, and hardness.

2. Experimental

2.1. Preparation of amorphous alloys

Thin Al–W films have been prepared by simultaneous deposition of pure metals sputtered in two independently controled cyllindrical magnetron sources [28]. The choice of deposition conditions has enabled the preparation of a wide range of films of varying chemical composition, from $\mathrm{Al}_{80}\mathrm{W}_{20}$ up to $\mathrm{Al}_{67}\mathrm{W}_{33}$. Films of 1 μm thickness have been deposited on sapphire disk-shaped substrates of 1 cm diameter. 16 samples have been prepared and divided intro three groups, depending on the chemical composition of the film: $\mathrm{Al}_{80}\mathrm{W}_{20}$, $\mathrm{Al}_{75}\mathrm{W}_{25}$ and $\mathrm{Al}_{67}\mathrm{W}_{33}$. Before and after exposure to corrosive solution, the structure and morphology of prepared films have been investigated by X-ray diffraction and optical microscopy.

The measured hardness of amorphous films amounted to 7.5 GPa, which is greater than that observed for pure tungsten. The films also exhibited thermal stability of the amorphous phase up to the temperatures in the range from 550 to 650 °C (depending on the composition).

The structure of prepared films has been determined by X-ray diffraction using a vertical goniometer Philips PW 1820. The morphology of film surface was checked by optical microscopy.

Corrosion resistance of protective films was investigated in an artificial saliva solution, $\mathrm{pH} = 5.5$ (NaCl 0.4 g/l; KCl 0.4 g/l; $\mathrm{CaCl} \times 2\mathrm{H_2O}$ 0.795 g/l; $\mathrm{NaH_2PO_4}$ 0.7 g/l; urea 1.0 g/l) at a temperature of 20 °C, using electrochemical techniques: cyclic voltammetry and linear polarization.

2.2. Equipment used in corrosion measurements

The equipment used in corrosion measurements consisted of an electrochemical cell with computer controled potentiostat/galvanostat (Electrochemical Interface, Solartron SI 1287) using the software: CorrWare, CorrView, Scribner Associates, Inc. support: Derek Johnson, 1997.

Electrochemical measurements were performed in a three-electrode cell, the Corrosion Cell System Model K47, Princeton Applied Research (PAR). The cell volume amounted to 1 dm^3. The working electrode was situated in the central opening, the counter electrodes were symmetrically positioned on each side, and the reference electrode was diagonally positioned across from the working electrode.

2.2.1. Working electrode

Amorphous films of composition $\mathrm{Al}_{80}\mathrm{W}_{20}$, $\mathrm{Al}_{75}\mathrm{W}_{25}$ and $\mathrm{Al}_{67}\mathrm{W}_{33}$ on a disk-shaped sapphire substrate were nested in a teflon holder, so that the exposed surface of the sample amounted to 1 cm^2. Prior to each measurement, the electrodes were degreased with ethanol.

2.2.2. Reference electrode

Saturated calomel electrode (SCE: $\mathrm{Hg/Hg_2Cl_2}$ in saturated KCl) with the potential 0.224 V more positive than the potential of the standard hydrogen electrode, SHE. The reference electrode was placed in a glass tube filled with saturated KCl solution, with a capillary in the end. The electrical contact between the electrolyte and the reference electrode was, established through a porous sintered piece of glass at the end of the capillary. All potential values in this paper are referred to the saturated calomel electrode, SCE.

2.2.3. Counter electrodes

Two graphite rods were employed, situated symmetrically across from the working electrode, in order to achieve a uniform distribution of the currents.

3. Results

3.1. Time change of the corrosion potential

Prior to the electrochemical tests of corrosion behavior of Al–W amorphous alloys and their individual compo-

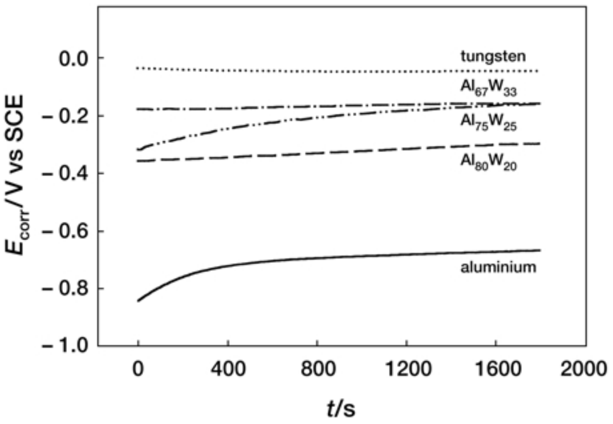

Figure 1 The time change of the corrosion potential, E_{corr} for aluminum, tungsten and Al–W alloy in saliva solution (pH = 5.5).

nents, it was important to determine the time necessary to establish the stationary state in the system alloy | simulated saliva solution, pH = 5.5, at the open circuit potential, $E_{OCP} = E_{corr}$. From Fig. 1, which shows the change in E_{OCP} with time of exposure of Al, W and Al–W alloys to the biosurroundings, it is evident that for most investigated alloys, the corrosion potential attained a value that did not change during 2000 s. It is obvious from the figure that pure aluminum has the most negative E_{corr}, while tungsten has the most positive E_{corr}, and that, with an increase in tungsten contribution in the amorphous Al–W coating, the corrosion potential becomes more positive.

3.2. Determination of the corrosion rate from polarization resistance measurements

The method used to determine the rate of corrosion of investigated materials from polarization resistance, employed in this work, is the method which suits the real application conditions of the investigated system, because the amplitude of the alternating signal amounts to ± 5 mV from E_{corr} so the departure of the system from the stationary state is negligible. The Tafel method, on the contrary, requires a significantly larger amplitude of the perturbation signal (± several hundred millivolts from E_{corr}), which might influence the accuracy of the results due to a change in the surface state. The polarization resistance is a measure of the metal resistance to corrosion and is defined by the slope of the potential-current curve in the near vicinity of the corrosion potential ($E = E_{corr} \pm 5$ mV). The current–potential relationship in this region is linear [29]. The polarization resistance value, R_p is determined from the equation $\Delta E = E - E_{corr}$ and the corresponding change in the current, ΔI according to the relation:

$$R_p = A\frac{\Delta E}{\Delta I} \tag{1}$$

where A is the surface of the electrode.

The Stern and Geary equation based on the Wagner–Traud kinetic principle ($\Sigma j_a = \Sigma j_c = j_{corr}$ at the potential, E_{corr}) enables the calculation of the corrosion current using experimentally determined values of polarization resistance, R_p [12, 30]:

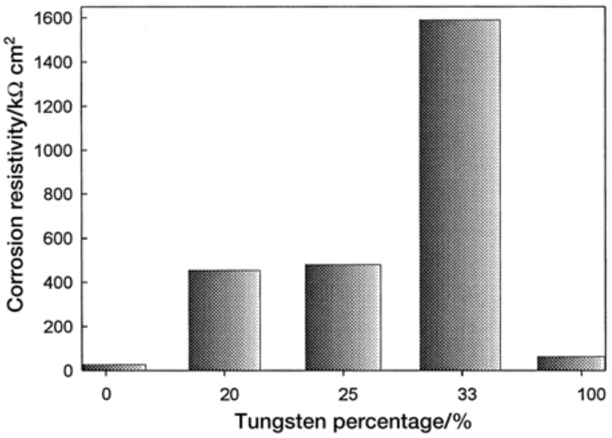

Figure 2 The corrosion resistance of aluminum, tungsten and Al–W alloy in artificial saliva solution (pH = 5.5) obtained from the polarization measurements and calculated according to Equation 1.

$$j_{corr} = \frac{B}{R_p}\ B = \frac{b_a b_c}{2303(b_a + b_c)} \tag{2}$$

where j_{corr} is the corrosion current density, while b_a and b_c are the Tafel slopes for the anodic and the cathodic process, respectively. Their values were taken from our unpublished results and correspond to: $b_a = 150$ mV, $b_c = 70$ mV, and $B = 20$ mV. From the corrosion current densities, j_{corr} determined according to Equation 2, the rate of corrosion was calculated, ν_{corr} in terms of the loss of mass per unit area during one year, according to the Faraday law:

$$\nu_{corr} = \frac{j_{corr}M}{zF} \tag{3}$$

where M is the molar mass of the alloy obtained from atomic contributions of alloy components, z is the number of exchanged electrons, and F is the Faraday constant. Fig. 2 shows histograms representing the polarization resistance values, R_{p}, that is, the corrosion resistance of investigated materials in artificial saliva solution.

The diagrams in Fig. 3 show the dependence of the corrosion potential, E_{corr} and the rate of corrosion, ν_{corr}, on tungsten content in the Al–W alloy in artificial saliva solution.

The values of kinetic corrosion parameters R_p and j_{corr} calculated using the software CorrView are contained in

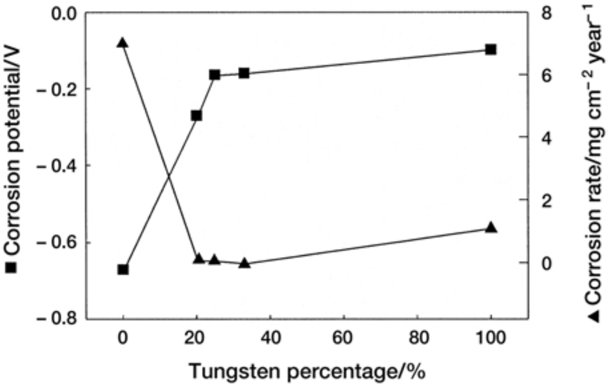

Figure 3 The dependence of the corrosion potential, E_{corr} and the corrosion rate, ν_{corr} (calculated according to Equation 3) on the tungsten content in the alloy immersed in artificial saliva solution (pH = 5.5).

TABLE I Corrosion parameters obtained on aluminum, tungsten and amorphous alloy $Al_{67}W_{33}$, $Al_{75}W_{25}$, $Al_{80}W_{20}$ electrodes in artificial saliva solution (pH = 5.5)

	R_p/kΩ cm^2	j_{corr}/10^{-8}A cm^{-2}	v/mg cm^{-2} y^{-1}	E_b/V	E_{rp}/V
Al	8.4	238.00	7.00	− 0.4	− 0.7
$Al_{80}W_{20}$	460.0	4.34	0.16	0.8	0.3
$Al_{75}W_{25}$	488.0	4.10	0.13	1.1	0.7
$Al_{67}W_{33}$	1590.0	1.25	0.06	1.4	1.2
W	30.9	64.70	1.08	—	—

Table I. Very small corrosion currents, of the order of 10^{-8} A/cm^2, may be observed from the table for amorphous Al–W, as a result of the presence of a passive oxide film. This film, which spontaneously forms in contact with the electrolyte, isolates the alloys from the aggressive influence of the medium (artificial saliva) and makes them very stable.

3.3. Anodic behavior of amorphous Al–W alloys; determination of critical pitting corrosion parameters

Passive films are susceptible to localized damage caused by mechanical (stretching of the passive film with respect to the substrate, thermal stress, solution flow, cavitation) and/or chemical effects. The best known cause of localized dissolution and localized oxide film breakdown is initiated by specific adsorption of chloride ions, which are present in the artificial saliva solution at a concentration of $c(\mathrm{Cl}^-) \approx 0.8\ \mathrm{g\,l}^{-1}$.

The susceptibility of thin amorphous Al–W films to localized pitting corrosion, as dependent on alloy composition, was investigated using cyclic voltammetry. In Fig. 4, the anodic portion of the current cycle recorded on aluminum and tungsten may be seen, while Figs. 5–7 show the cyclic voltammograms for Al–W electrodes. Electrochemical behavior of Al–W alloys is characterized by a wide passive region (where the current is independent of potential), which ends with a sharp increase in current. The potential at which this sudden change in current and the rate of reaction take place corresponds to the critical oxide film breakdown potential, E_b, that is, the pitting potential, E_{pit}. In the return current cycle, the potential at which the ionic current of metal dissolution attains a value of zero corresponds to the repassivation potential, E_{rp}. From the polarization curves and the results contained in Table I, it is obvious that with an increase in tungsten content in the alloy, the pitting and repassivation potentials shift toward more positive values, and that the potential region in which the electrode remains passive, expands. Between the potentials E_{rp} and E_b (the surface of the anodic loop), a stochastic process of pit initiation takes place, and at potentials more positive than E_b, the pits expand and penetrate deeper into the material, which ends with generalized corrosion at $E \gg E_b$.

According to the PDM [31–33], Table I, the following corrosion processes take place at the interphase boundary

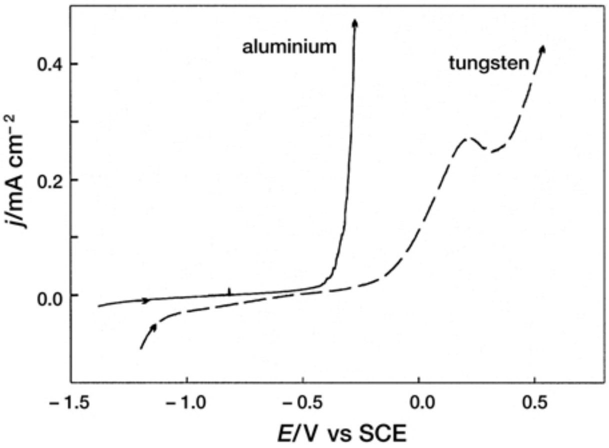

Figure 4 Polarization diagrams recorded on aluminum and tungsten electrodes in artificial saliva solution (pH = 5.5), at a potential scan rate of 10 mV/s.

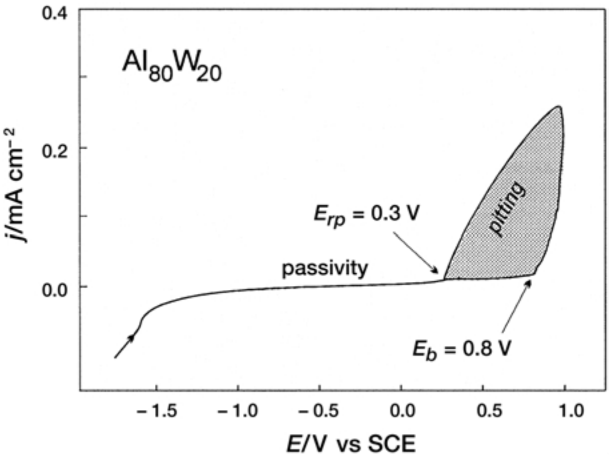

Figure 5 Cyclic voltammogram recorded on the $Al_{80}W_{20}$ electrode in artificial saliva solution (pH = 5.5), at the potential scan rate of 10 mV/s.

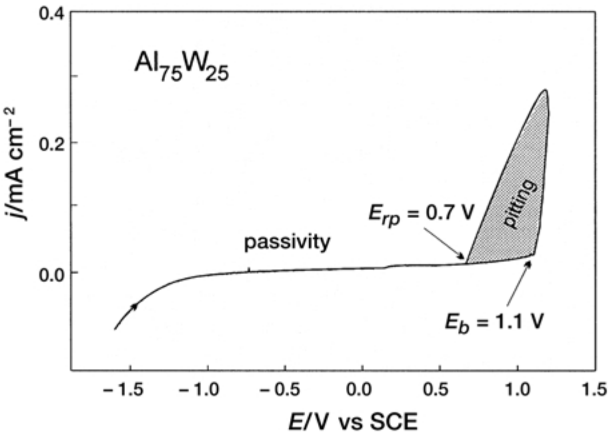

Figure 6 Cyclic voltammogram recorded on the $Al_{75}W_{25}$ electrode in artificial saliva solution (pH = 5.5), at the potential scan rate of 10 mV/s.

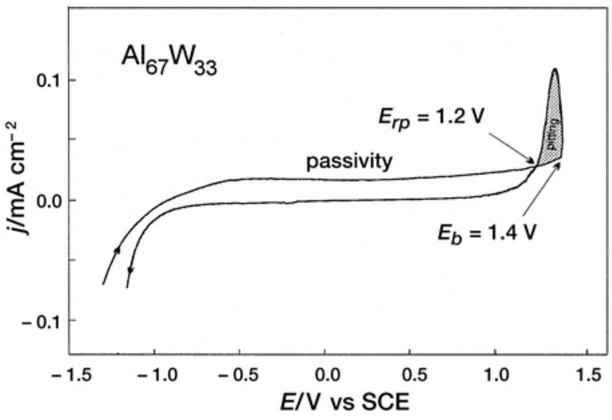

Figure 7 Cyclic voltammogram recorded on the $Al_{67}W_{33}$ electrode in artificial saliva solution (pH = 5.5), at the potential scan rate of 10 mV/s.

oxide film | electrolyte: (i) the transfer of cations from the oxide lattice into the electrolyte solution and the formation of cation vacancies $V_M^{\chi'}$ according to reaction (4) [33], (ii) adsorption of Cl^- ions from the solution into anion vacancies at the interphase boundary oxide film|electrolyte and the formation of positively charged $Cl_o^{\bullet}$ chloride ion according to reaction (5). The system responds to the loss of an anion vacancy by forming a new pair of the cation and anion (oxygen) vacancies according to the Schottky reaction (6) [33].

$$M_M \rightarrow M^{\delta+}(aq) + V_M^{\chi'} + (\delta - \chi)e \qquad (4)$$

$$X^- \cdot nH_2O + V_{\ddot{O}}(ox) \longleftrightarrow X_O^{\bullet}(ox) + nH_2O \qquad (5)$$

Mott–Schottky pair reaction:

$$X^- \cdot nH_2O + (V_{\ddot{O}} \cdot V_M^{\chi'}) + M_M^{\chi+} \qquad (6)$$

where X^- is a nucleophilic anion (Cl^-), $X_o^{\bullet}$ is a positively charged nucleophilic anion adsorbed in the anion vacancy, $V_{\ddot{O}}$, and $V_M^{\chi'}$ is the cation vacancy.

The oxygen vacancies formed according to relation (6) react again with additional Cl^- ions at the interphase boundary film|solution (autocatalytic effect), while the cation vacancies $V_M^{\chi'}$ diffuse through the oxide film to the interphase boundary metal | oxide film, where they become cancelled by the cations entering the vacancy. If the rate of cation vacancies diffusion is greater than the rate of cation cancellation, then the uncancelled cation vacancies will accumulate at the interphase boundary metal|oxide, forming condensates, which, upon reaching the critical value, cause the separation of the barrier layer from the substrate metal. Film breakdown initiates the formation of pits and the onset of pitting corrosion. In this case, the alloy dissolves locally, due to the effects of small anodic current and a large cathodic surface.

The idea according to which the diffusion of cationic vacancies through the oxide layer plays the most important role in the susceptibility of alloys to pitting corrosion was applied by Urquidi-Macdonald and Macdonald [34, 35] for the prediction of the role of alloying elements in modifying the corrosion resistance of the alloys. The assumption of their model of alloying element interactions with the vacancies (solute-vacancy interaction model; SVIM) is the formation of pairs (complexing) between the immobile alloying element ions in the highest oxidation state and the mobile cation vacancies. The interaction of the alloying ion and the mobile cation vacancy may be in general, described by the ''complexing'' equation:

$$M_M^{(\delta-\chi)+} + q V_M^{\chi'} \overset{K_q}{\longleftrightarrow} [M_M(V_M^{\chi'})q]^{[\delta-\chi(1+q)]} \qquad (7)$$

The investigation of the composition and structure of galvanostatically [36, 37] and potentiodynamically [37–40] formed oxide films on Al–W amorphous alloys, in the wide pH range of electrolyte solutions, showed that the passivation process takes place in two stages. In the initial stage, a pure aluminum oxide (alumina) forms while tungsten segregates underneath this layer, at the interphase boundary alloy | oxide film. This may be explained by a high affinity of aluminum for the oxygen, that is, by the formation of strong metal–oxygen bonds, while tungsten strengthens the metal bonds in the alloy and prevents its dissolution – corrosion [41]. In the second passivation stage, under the influence of the electric field, tungsten integrates into the cation vacancies of aluminum in the form of W^{6+}, according to the reaction (8):

$$W_W(m) + V_{Al}^{3'} \longleftrightarrow W_{Al}^{3\bullet} + 3e \qquad (8)$$

$W_{Al}^{3\bullet}$ is formally the carrier of three positive charges, which forms a neutral complex by electrostatically interacting with a negatively charged aluminum vacancy:

$$W_{Al}^{3\bullet} + V_{Al}^{3'} \longleftrightarrow [W_{Al} \cdot V_{Al}] \qquad (9)$$

It is therefore plausible to expect that with an increase in tungsten content in the alloy, the concentration of cation vacancies will decrease and cause an increase in corrosion resistance of the material. It is obvious from Table I that the breakdown potential, E_b shifts towards more positive potential values, as well as the repassivation potential, E_{rp}. At the same, time, the corrosion current density and the rate of generalized corrosion decrease with an increase in tungsten content in the alloy.

4. Conclusions

On the basis of accelerated corrosion tests performed in the artificial saliva solution, pH = 5.5, using electrochemical methods, the following conclusions can be drawn.

Thin amorphous Al–W films deposited on a sapphire substrate by magnetron codeposition exhibit excellent corrosion resistivity in artificial saliva, which is very demanding for materials used in dentistry.

Exceptional corrosion stability of Al–W amorphous alloys may be explained by semiconductor characteristics of the nonstoichiometric oxide film spontaneously formed or formed via anodic polarization in artificial saliva solution, pH = 5.5. Charge transfer through this film is achieved via point defects, anion and cation vacancies. Metal corrosion is related to the transfer of cations into the solution at the interphase boundary oxide (passive) film|solution and increased flux of cation vacancies $V_M^{\chi'}$ in the opposite direction, towards the film metal interphase boundary. However, after electrostatic interaction between the negatively charged cation vacancies and tungsten ions in the highest oxidation state (W^{6+}), neutral complexes form [Al–W], see Equation 9, and the material adopts isolator properties with very small corrosion currents, in the nanoampere range, and a negligible corrosion rate of the order of $10^{-4}\,\mathrm{g\,cm^{-2}\,yr^{-1}}$.

Since oxide films on metallic biomaterials are the fundamental condition governing biocompatibility of materials for dental (medical) applications, it may be concluded that amorphous Al–W alloys might find their application in oral prosthetics due to their durability and exceptional corrosion resistance.

List of symbols

R_p	Polarization resistance, $\Omega\,\mathrm{cm}^2$
A	Surface of the working electrode, cm^2
ΔE	Potential change, V
ΔI	Current change, A
j_{corr}	Corrosion current density, $\mathrm{A/cm^2}$
ν_{corr}	Corrosion rate, $\mathrm{g\,cm^{-2}\,yr^{-1}}$
E	Potential, V
E_{corr}	Corrosion potential, V
B	Constant, V
b_a	Anodic Tafel slope, V
b_c	Cathodic Tafel slope, V
χ	Cation vacancy charge
e	Unit charge, C
M_M	Metal cation in the oxide
$M^{\delta+}$(aq)	Metal cation in the solution
$V_M^{x'}$	Cation vacancy
$V_{\ddot{O}}$	Anion (oxygen) vacancy
X^-	Nucleophilic ion
$X_O^{\bullet}$	Halogen ion adsorbed in an anion vacancy

References

1. D. F. WILLIAMS (ed.), in ''Biocompatibility of Clinical Implant Materials'' (CRC Press. Inc. Boca Raton, Florida, 1981).
2. M. MAREK, *Mat. Sci. Technol.* **23** (1983) 331.
3. E. ANGELLINI, *J. Appl. Electrochem.* **28** (1998) 6.
4. E. C. MORENO and H. C. MARGOLIS, *J. Dent. Res.* **67** (1988) 1181.
5. K. LIAN and E. I. MELETIS, *Dent. Mater.* **12** (1996) 146.
6. J. MADDOX, *Nature* **327** (1987) 11.
7. D. E. POLK and B. C. GIESSEN, in ''Metallic Glasses'' (American Society for Metals, Ohio, 1978) p. 1.
8. M. D. ARCHER, C. C. CORKE and B. H. HARJI, *Electrochim. Acta* **32** (1987) 13.
9. T. MASUMOTO, K. HASHIMOTO and M. NAKA, in ''Rapidly Quenched Metals III'' (Elsevier Science Publishers, London, 1978) p. 435.
10. K. HASHIMOTO, in ''Rapidly Quenched Metals'' (Elsevier Science Publishers, New York, 1985) p. 1449.
11. D. LANDOLT, in ''Corrosion Mechanism in Theory and Practice'', edited by P. Marcus and J. Oudar (Marcel Dekker Inc., Hong Kong, Basel, New York, 1995) p. 1.
12. K. J. BUNDY, *Crit. Rev. Biomed. Eng.* **22** (1994) 139.
13. D. G. KOLMAN and J. R. SCULLY, *J. Electrochem. Soc.* **142** (1994) 2633.
14. M. A. KHAN, R. F. WILLIAMS and D. F. WILLIAMS, *Biomaterials* **17** (1996) 2117.
15. A. MARINOVIĆ, M. METIKOŠ-HUKOVIĆ and I. MILOŠEV in ''Electrochemical Approach to Selected Corrosion and Corrosion Control Studies'', edited by P. L. Bonora and F. Deflorian (IOM Communications, London, 2000) p. 166.
16. M. F. LOPEZ, A. GUTIERREZ and J. A. JIMENEZ, *Surf. Sci.* **482** (2001) 300
17. I. MILOŠEV, M. METIKOŠ-HUKOVIĆ and H.-H. STREHBLOW, *Biomaterials* **21** (2000) 2103.
18. Y.-S. LI, K. WANG, P. HE, B. X. HUANG and P. KOVACS, *J. Raman Spectrosc.* **30** (1999) 97.
19. T. HANAWA, S. HIROMOTO and K. ASAMI, *Appl. Surf. Sci.* **183** (2001) 68.
20. C.-O. OLSSON and D. LANDOLT, *J. Electrochem. Soc.* **148** (2001) B438.
21. N. E. HAKIKI, M. DA CUNHA BELO, A. M. P. SIMÕES and M. G. S. FERREIRA, *ibid.* **145** (1998) 3821.
22. I. MILOŠEV, *J. Appl. Electrochem.* **32** (2002) 311.
23. V. BRUSIĆ, in ''Oxides and Oxide Films'', edited by J. W. Diggle (Marcel Dekker, Inc., New York, 1972) p. 1.
24. D. D. MACDONALD, *Pure Appl. Chem.* **71** (1999) 951.
25. J. DOBEK, S. MROWEC and K. DANIELOWSKI, *Mater. Sci. Eng. A* **182** (1994) 1099.
26. K. HASLINAKA, *ibid. A* **33** (1991) 22.
27. K. HASHIMOTO, P. Y. PARK and J. H. KIM, *ibid. A* **198** (1995) 1.
28. N. RADIĆ, A. TONEJC, M. MILUN, P. PERVAN, J. IVKOV and M. STUBIČAR, *Thin Solid Films* **317** (1998) 96.
29. K. B. OLDHAM and F. MANSFELD, *Corros. Sci.* **13** (1973) 813.
30. N. M. G. FONTANA and N. D. GREENE, in ''Corrosion Engineering'' (Int. Student Editor, Tokyo, 1983) p. 499.
31. C. Y. CHAO, L. F. LIN and D. D. MACDONALD, *J. Electrochem. Soc.* **128** (1981) 1187.
32. D. D. MACDONALD, S. R. BIAGGIO and H. SONG, *ibid.* **139** (1992) 170.
33. D. D. MACDONALD, *ibid.* **139** (1992) 3434.
34. D. D. MACDONALD and M. URQUIDI-MACDONALD, *ibid.* **137** (1990) 2395.
35. D. D. MACDONALD and M. URQUIDI-MACDONALD, *ibid.* **132** (1985) 555.
36. H. HABAZAKI, P. SKELDON, G. E. THOMPSON, G. C. WOOD and K. SHIMIZU, *Philos. Mag. B* **71** (1995) 81.
37. A. WOLOWIK and M. JANIK-CZACHOR, *Mater. Sci. Eng. A* **267** (1999) 301.
38. H. YOSHIOKA, H. HABAZAKI, A. KAWASHIMA, K. ASAMI and K. HASHIMOTO, *Corros. Sci.* **32** (1991) 313 and 327.
39. G. D. DAVIS, B. A. SHAW, B. J. REES and M. FERRY, *J. Electrochem. Soc.* **140** (1993) 951.
40. M. METIKOŠ-HUKOVIĆ, N. RADIĆ, Z. GRUBAČ and A. TONEJC, *Electrochim. Acta* **47** (2002) 2387.
41. P. MARCUS, *ibid.* **43** (1998) 109.

Received 1 July 2002
and accepted 4 February 2003